Structure and Cytotoxic Activity of Enzymatic Hydrolysis Products of Secoiridoid Glucosides, Isoligustroside and Isooleuropein

by **Masafumi Kikuchi**[a])[b]), **Yasunori Yaoita**[b]), **Nariyasu Mano**[a]), and **Masao Kikuchi***[b])

[a]) Department of Pharmaceutical Sciences, Tohoku University Hospital, 1-1 Seiryo-machi, Aoba-ku, Sendai, Miyagi, 980-8547, Japan

[b]) Department of Molecular Structural Analysis, Tohoku Pharmaceutical University, 4-4-1 Komatsushima, Aoba-ku, Sendai, Miyagi 981-8558, Japan

(phone: +81-22-234-4181; fax: +81-22-275-2013; e-mail: mkikuchi@tohoku-pharm.ac.jp)

Hydrolysis of isoligustroside (**1**) and isooleuropein (**2**), secoiridoid glucosides, in the presence of β-glucosidase provided 2-(4-hydroxyphenyl)methyl (2*R*,3*S*,4*S*)-3-formyl-3,4-dihydro-4-(2-methoxy-2-oxoethyl)-2-methyl-2*H*-pyran-5-carboxylate (**3**) and 2-(3,4-dihydroxyphenyl)methyl (2*R*,3*S*,4*S*)-3-formyl-3,4-dihydro-4-(2-methoxy-2-oxoethyl)-2-methyl-2*H*-pyran-5-carboxylate (**4**), respectively. The structures of **3** and **4** were elucidated on the basis of extensive spectral analyses, including 2D-NMR experiments. Compounds **3** and **4** were found to be new rearrangement products of the aglycones of **1** and **2**. The cytotoxic activities of **3** and **4** were evaluated using a disease-oriented panel of 39 human cancer cell lines and showed moderate cytotoxic activity for **4**, while **3** exhibited weaker activity compared to that of **4**.

Introduction. – Lilacs (*Syringa*) are a genus of *ca.* 20 species of flowering plants in the family Oleaceae, and they are used as antimicrobial, antipyretic, and antivirus medicines. In a previous article, we reported the isolation and structure elucidation of secoiridoid glucosides isoligustroside (**1**) and isooleuropein (**2**) from the leaves of *S. vulgaris* L. [1]. It has been reported that the aglycones, obtained by treatment of secoiridoid glucosides, gentiopicroside and sweroside, with β-glucosidase, exhibited antitumor activities; however, gentiopicroside and sweroside did not display this activity [2]. These observations indicated that these secoiridoid glucosides possess bioactivities after only deglucosidation [3]. This prompted us to investigate the bioactivity of the enzymatic hydrolysis products of **1** and **2**. Here, we describe the structure and cytotoxic activity of the products **3** and **4**, obtained from the enzymatic hydrolysis of **1** and **2** with β-glucosidase.

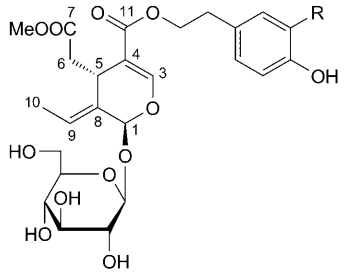

1 R = H
2 R = OH

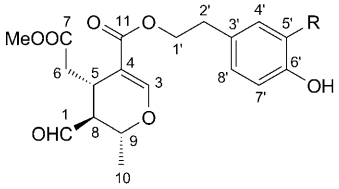

3 R = H
4 R = OH

Results and Discussion. – 1. *Enzymatic Hydrolysis and Structure Elucidation*. Hydrolysis of compounds **1** and **2** in the presence of β-glucosidase provided compounds **3** and **4** in 20 and 25% yield, respectively. The reaction conditions of *Guiso* and *Marra* [4] were adopted, *i.e.*, a solution of the substrate in H_2O was treated with an excess of β-glucosidase at 34°.

Compound **3** was obtained as an amorphous powder. Its molecular formula was determined as $C_{19}H_{22}O_7$ based on HR-EI-MS (*m/z* 362.1367 (M^+; calc. 362.1365)). The UV spectrum suggested the presence of an enol-ether system conjugated with a CO group (232 nm), which is typical for many iridoid and secoiridoid skeletons [5]. In addition, absorption due to a phenol chromophore (276 nm) was also observed. The ^{1}H-NMR spectrum of **3** (in $CDCl_3$; *Table 1*) exhibited signals due to one Me group (δ(H) 1.42 (*d*, *J* = 6.6)), one MeO group (δ(H) 3.66 (*s*)), one O-bearing CH group (δ(H) 4.43 (*dq*, *J* = 6.6, 6.2)), one C=C–H moiety (δ(H) 7.45 (*s*)), and one aldehyde H-atom (δ(H) 9.61 (*d*, *J* = 1.8)). The ^{1}H-NMR spectrum also indicated the presence of a *p*-substituted aromatic ring. The ^{13}C-NMR spectrum of **3** (in $CDCl_3$; *Table 1*) displayed signals due to three C=O groups (δ(C) 166.5, 172.4, and 199.9). The ^{1}H,^{1}H-COSY spectrum of **3** (*Fig. 1*) implied connectivities of H–C(1) to H–C(8)[1]), of H–C(5) to CH_2(6), of H–C(5) to H–C(8), of H–C(8) to H–C(9), of H–C(9) to Me(10), of CH_2(1′) to CH_2(2′), of H–C(4′) to H–C(5′), and of H–C(7′) to H–C(8′). The HMBC

Table 1. *^{1}H-* (600 MHz) *and ^{13}C-NMR* (150 MHz) *Data of Compounds* **3** *and* **4** *in $CDCl_3$*[1]). δ in ppm, *J* in Hz.

	3		**4**	
	δ(H)	δ(C)	δ(H)	δ(C)
H–C(1)	9.61 (*d*, *J* = 1.8)	199.9	9.60 (*s*)	200.0
H–C(3)	7.54 (*s*)	155.4	7.56 (*s*)	155.7
C(4)	–	106.7	–	106.5
H–C(5)	3.38–3.40 (*m*)	27.2	3.42–3.43 (*m*)	27.0
CH_2(6)	2.50 (*dd*, *J* = 16.1, 9.5), 2.85 (*dd*, *J* = 16.1, 3.7)	36.8	2.55 (*dd*, *J* = 16.1, 9.9), 2.84–2.88 (*m*)	37.0
C(7)	–	172.4	–	173.0
H–C(8)	2.68 (*ddd*, *J* = 6.2, 5.9, 1.8)	54.7	2.65–2.67 (*m*)	54.5
H–C(9)	4.43 (*dq*, *J* = 6.6, 6.2)	70.8	4.47 (*dq*, *J* = 6.6, 6.2)	70.7
Me(10)	1.42 (*d*, *J* = 6.6)	19.4	1.42 (*d*, *J* = 6.6)	19.4
C(11)	–	166.5	–	166.7
CH_2(1′)	4.28–4.33 (*m*)	64.9	4.30–4.32 (*m*)	65.1
CH_2(2′)	2.88–2.90 (*m*)	34.3	2.84–2.88 (*m*)	34.4
C(3′)	–	130.02	–	130.6
H–C(4′)	7.08 (*d*, *J* = 8.1)	130.04	6.80 (*s*)	115.3
H–C(5′)	6.77 (*d*, *J* = 8.1)	115.4	–	143.5
C(6′)	–	154.3	–	142.7
H–C(7′)	6.77 (*d*, *J* = 8.1)	115.4	6.75–6.80 (*m*)	116.1
H–C(8′)	7.08 (*d*, *J* = 8.1)	130.04	6.62 (*d*, *J* = 7.0)	121.2
MeO	3.66 (*s*)	51.8	3.69 (*s*)	52.1

[1]) Arbitrary numbering, see *Formulae*. For systematic names, see *Exper Part*.

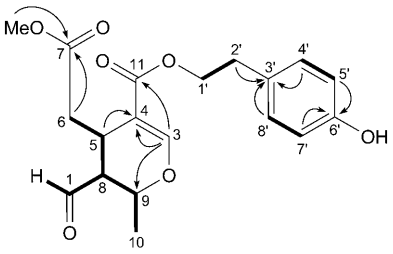

Fig. 1. *$^1H,^1H$-COSY* (bold lines) *and HMBC* (full-line arrows) *correlations for* **3**

spectrum (*Fig. 1*) showed the correlations H–C(3)/C(4), C(9), and C(11); H–C(5)/C(4); CH_2(6)/C(7); CH_2(2′)/C(3′); H–C(4′)/C(3′); H–C(5′)/C(6′); H–C(7′)/C(6′); H–C(8′)/C(3′), and MeO/C(7). By considering the chemical shift of C(11) (δ(C) 166.5), the linkage position of the 2-(4-hydroxyphenyl)ethoxy group was determined as C(11), affording the constitution of **3**. The relative configuration of **3** was determined as follows. In the ^{1}H-NMR spectrum, H–C(8) had a large coupling constant ($J(8\alpha,9\beta) =$ 6.2). In an NOESY experiment, NOE correlations H–C(1)/H–C(5), H–C(5)/H–C(9), and H–C(8)/Me(10), were observed revealing that **3** adopted a conformation as shown in *Fig. 2*, and the CH_2COOMe group at C(5), the CHO group at C(8), and Me(10) were α-, β-, and α-oriented, respectively (*Fig. 2*). The absolute configuration of **3** was determined as (5*S*,8*S*,9*R*)[1]) by the positive $[\alpha]_D$ value [6]. Accordingly, the structure of **3** was elucidated as 2-(4-hydroxyphenyl)ethyl (2*R*,3*S*,4*S*)-3-formyl-3,4-dihydro-4-(2-methoxy-2-oxoethyl)-2-methyl-2*H*-pyran-5-carboxylate.

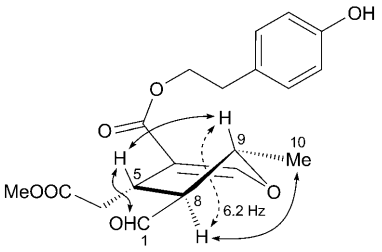

Fig. 2. *Selected coupling constant* (dotted arrow) *and NOESY* (full-line arrows) *correlations for* **3**

Compound **4** was obtained as an amorphous powder. The general features of ^{1}H- and ^{13}C-NMR spectra of **4** (in $CDCl_3$; *Table 1*) closely resembled those of **3** except that one of the aromatic H-atoms in ^{1}H-NMR spectrum of **4** was missing. The molecular formula was determined as $C_{19}H_{22}O_8$ based on HR-EI-MS (*m*/*z* 378.1318 (M^+; calc. 378.1315)). Consequently, **4** was deduced to be a compound in which an aromatic H-atom in **3** was replaced by an OH group. The resonance for C(5′) at δ(C) 115.4 of **3** was shifted downfield to δ(C) 143.5 in **4**, suggesting that an additional OH group was located at C(5′) [7]. This was confirmed by the HMBC spectrum, in which the cross-peak H–C(4′)/C(5′) was observed. The absolute configuration of **4** was determined as (5*S*,8*S*,9*R*)[1]) by the positive $[\alpha]_D$ value [6]. From these data, the structure of **4** was elucidated as 2-(3,4-dihydroxyphenyl)ethyl (2*R*,3*S*,4*S*)-3-formyl-3,4-dihydro-4-(2-methoxy-2-oxoethyl)-2-methyl-2*H*-pyran-5-carboxylate.

A proposed pathway for the formation of **3** and **4** is depicted in the *Scheme*. The aglycones **5** and **6**, resulting from the enzymatic hydrolysis of the glucosidic linkage of **1** and **2**, respectively, are in equilibrium with **7** and **8**, respectively. Compounds **3** and **4** are formed from **7** and **8**, respectively, by *Michael*-type addition [6][8]. Thus, a rearrangement of the dihydropyran ring of **5** and **6** occurs during the enzymatic hydrolysis. Compounds **3** and **4** were found to be new rearrangement products of aglycones.

Scheme

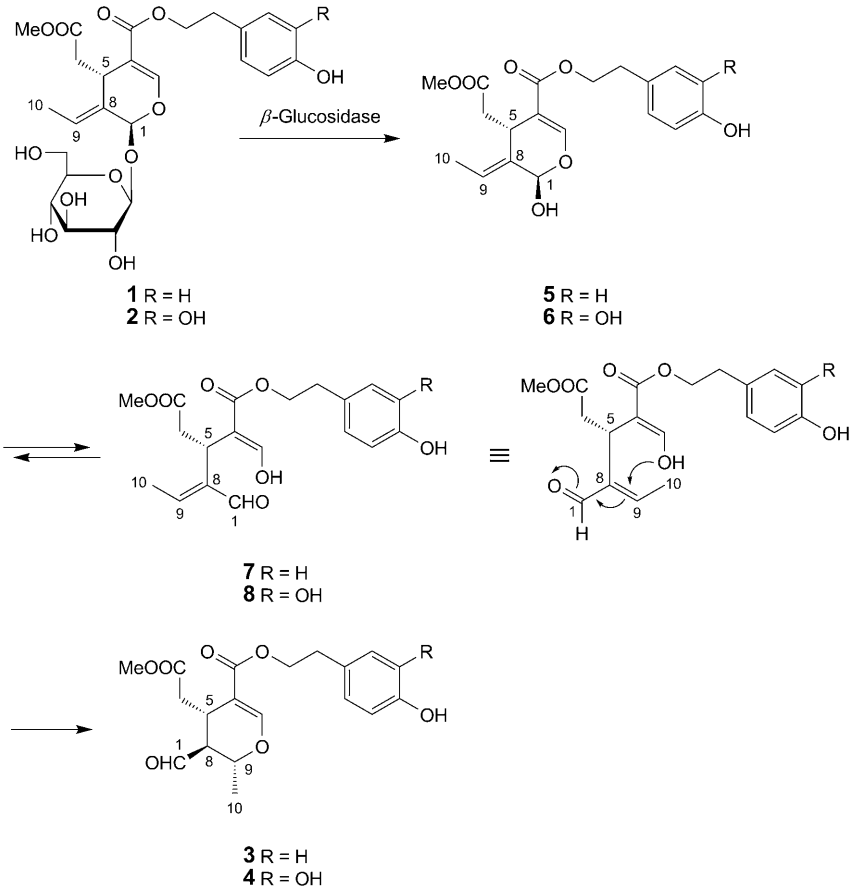

2. *Growth Inhibition against a Panel of 39 Human Cancer Cell Lines.* To evaluate compounds for their cell growth inhibition profile, a human cancer cell line panel combined with a database was established by the *Cancer Chemotherapy Center* of the *Japanese Foundation for Cancer Research* [9]. The system as a whole was developed according to the method of the *National Cancer Institute*, with modifications [10]. The cell-line panel consisted of 39 human cancer cell lines (five breast, six central nervous system, five colon, seven lung, one melanoma, five ovary, two kidney, six stomach, and two prostate cancers). The cancer growth inhibitory properties of **3** and **4** were

examined using a disease-oriented panel of 39 human cancer cell lines. The results are presented in *Table 2* as log GI_{50} (logarithmic concentration of compound for inhibition of cell growth at 50% relative to control) and GI_{50} (concentration of compound for inhibition of cell growth at 50% relative to control) values. Compound **4** showed significant cytotoxic activity against the lung cancer DMS273 (log GI_{50} −5.19 (6.4 μM)) and DMS114 (log GI_{50} −5.06 (8.7 μM)) cell lines, and the average logarithm of the GI_{50} (MG-MID) across all cell lines tested was −4.66 (22 μM). The MG-MID value of **3** was −4.41 (39 μM). These data disclosed that **4** showed moderate cytotoxic activity, while **3** was weaker in activity compared to **4**. It is noteworthy that the OH group at C(5′) of **4** is important to enhance the cytotoxic activity. The Δ value (the difference in log GI_{50} value between the most sensitive cell and the MG-MID value) and range value (the difference in the log GI_{50} value between the most and least sensitive cells) have been employed as a criterion for the selective cytotoxic activity (effective value: $\Delta \geq 0.5$ as well as range ≥ 1.0) [9]. As shown in *Table 2*, the Δ and range values of **4** were 0.54 and 1.19, respectively, indicating that **4** exhibited selective cytotoxic activity. On the other hand, **3** did not show selective cytotoxic activity ($\Delta = 0.40$, range = 0.81). Most anticancer agents with the same mechanism of action display similar cell growth inhibition profiles against a cancer cell line database. The cell growth inhibition profiles of **3** and **4** were submitted to data analysis by the COMPARE program [10], a database covering cell growth inhibition profiles of over 200 known anticancer agents with various action mechanisms. This program can be used to predict the mode of action of test compounds by assessing the correlation coefficient (r) between the cell growth inhibition profiles mediated by such test compounds and various reference compounds with known modes of action. The highest r values of **3** and **4** were realized with 6-sulfanylpurine ($r = 0.601$), a purine antagonists, for **3**, and nitrogen mustard ($r = 0.574$), a DNA alkylating agent, for **4**, respectively, suggesting that the modes of action of **3** and **4** are similar to those of the respective anticancer agents.

We are grateful to Dr. *T. Yamori* (*Screening Committee of Anticancer Drugs* supported by a *Grant-in-Aid for Scientific Research on Priority Area 'Cancer'* from the *Ministry of Education, Culture, Sports, Science and Technology*, Japan) for performing the assay for cytotoxicity using a panel of 39 human cancer cell lines. We are also grateful to Mr. *S. Satoh* and Mr. *T. Matsuki* of Tohoku Pharmaceutical University for NMR and MS recordings.

Experimental Part

General. HPLC: *CCPD* pump (*Tosoh*) and *UV-8011* UV/VIS detector (*Tosoh*); t_R in min. Optical rotations: *JASCO DIP-360* digital polarimeter. UV Spectra: *Beckman DU-64* spectrophotometer. NMR Spectra: *JEOL JNM-LA 600* (^{1}H: 600 MHz; ^{13}C: 150 MHz) spectrometer; chemical shifts δ in ppm, rel. to Me_4Si, J in Hz. EI-MS: *JEOL JMS-DX 303* mass spectrometer; in m/z.

Substrate Material. Isoligustroside (**1**) and isooleuropein (**2**) were isolated from the leaves of *Syringa vulgaris*, and characterized by spectroscopic methods as described in [1].

Enzymatic Hydrolysis of **1** *and* **2** *with β-Glucosidase.* Compound **1** (25 mg) was dissolved in H_2O (5.0 ml). The soln. was treated with an excess of β-glucosidase (from almonds; 15.3 units/mg; *Toyobo Corporation*) for 1 d at 34°. The soln. was then extracted with an equal amount of $CHCl_3$ (3×), and the $CHCl_3$ layer was evaporated under reduced pressure. The residue was purified by prep. HPLC (*Cosmosil 5SL-II* column (250 × 10 mm, 10 μm; *Nacalai Tesque*); $CHCl_3$/hexane/MeOH/AcOH 55 : 45 : 4 : 2, 1.0 ml/min) to give **3** (3.5 mg, t_R 24.0). By a similar procedure except the prep. HPLC conditions (*Cosmosil 5SL-*

Table 2. *Growth-Inhibition Activities of Compounds* **3** *and* **4** *against a Panel of 39 Human Cancer Cell Lines*

Type of cancer	Cell line	**3**		**4**	
		log GI_{50} [M][a])	GI_{50} [μM][b])	log GI_{50} [M]	GI_{50} [μM]
Breast	HBC-4	−4.32	48	−4.67	21
	BSY-1	−4.25	56	−4.71	19
	HBC-5	−4.42	38	−4.72	19
	MCF-7	−4.44	36	−4.66	22
	MDA-MB-231	−4.38	42	−4.74	18
Central nervous system (brain)	U251	−4.34	46	−4.63	24
	SF-268	−4.28	52	−4.67	21
	SF-295	−4.43	38	−4.54	29
	SF-539	−4.56	28	−4.74	18
	SNB-75	−4.46	34	−4.69	21
	SNB-78	−4.36	44	−4.62	24
Colon	HCC2998	−4.51	31	−4.76	17
	KM-12	−4.35	45	−4.61	25
	HT-29	−4.40	40	−4.50	32
	HCT-15	−4.37	42	−4.65	22
	HCT-116	−4.44	37	−4.61	25
Lung	NCI-H23	−4.37	43	−4.57	27
	NCI-H226	−4.49	33	−4.62	24
	NCI-H522	−4.81	16	−4.95	11
	NCI-H460	−4.21	62	−4.53	29
	A549	−4.00	>100	−4.00	>100
	DMS273	−4.77	17	−5.19	6.4
	DMS114	−4.58	26	−5.06	8.7
Melanoma	LOX-IMVI	−4.54	29	−4.74	18
Ovary	OVCAR-3	−4.71	19	−4.74	18
	OVCAR-4	−4.21	61	−4.65	22
	OVCAR-5	−4.46	35	−4.68	21
	OVCAR-8	−4.44	36	−4.55	28
	SK-OV-3	−4.27	54	−4.58	26
Kidney	RXF-631L	−4.53	30	−4.62	24
	ACHN	−4.32	48	−4.70	20
Stomach	St-4	−4.47	34	−4.55	28
	MKN1	−4.44	36	−4.78	16
	MKN7	−4.40	40	−4.61	25
	MKN28	−4.39	41	−4.57	27
	MKN45	−4.31	48	−4.65	22
	MKN74	−4.40	40	−4.62	24
Prostate	DU-145	−4.07	85	−4.56	28
	PC-3	−4.35	44	−4.59	26
MG-MID[c])		−4.41		−4.66	
Δ[d])		0.40		0.54	
Range[e])		0.81		1.19	

[a]) Logarithmic concentration of compound for inhibition of cell growth at 50% relative to control. [b]) Concentration of compound for inhibition of cell growth at 50% relative to control. [c]) Mean value of log GI_{50} over all cell lines tested. [d]) Difference in log GI_{50} value between the most sensitive cell and the MG-MID value. [e]) Difference in log GI_{50} value between the most and least sensitive cells.

II column (250 × 10 mm, 10 μm, *Nacalai Tesque*); $CHCl_3$/hexane/MeOH/AcOH 55 : 45 : 4 : 1, 1.0 ml/min), **4** (9.8 mg, t_R 30.6) was obtained from **2** (55 mg).

*2-(4-Hydroxyphenyl)ethyl (2*R*,3*S*,4*S*)-3-Formyl-3,4-dihydro-4-(2-methoxy-2-oxoethyl)-2-methyl-2*H*-pyran-5-carboxylate* (**3**). Amorphous powder. $[\alpha]_D^{25} = +30.9$ ($c = 0.35$, $CHCl_3$). UV (MeOH): 232 (4.2), 276 (3.3). ^{1}H- and ^{13}C-NMR: see *Table 1*. EI-MS: 362 (M^+). HR-EI-MS: 362.1367 (M^+, $C_{19}H_{22}O_7^+$; calc. 362.1365).

*2-(3,4-Dihydroxyphenyl)ethyl (2*R*,3*S*,4*S*)-3-Formyl-3,4-dihydro-4-(2-methoxy-2-oxoethyl)-2-methyl-2*H*-pyran-5-carboxylate* (**4**). Amorphous powder. $[\alpha]_D^{27} = +31.0$ ($c = 0.98$, $CHCl_3$). UV (MeOH): 231 (4.5), 281 (3.8). ^{1}H- and ^{13}C-NMR: see *Table 1*. EI-MS: 378 (M^+). HR-EI-MS: 378.1318 (M^+, $C_{19}H_{22}O_8^+$; calc. 378.1315).

Cell Growth-Inhibition Assay. This experiment was carried out at the *Cancer Chemotherapy Center* of the *Japanese Foundation for Cancer Research*. The screening panel consisted of the following 39 human cancer cell lines: breast cancer HBC-4, BSY-1, HBC-5, MCF-7, and MDA-MB-231; brain cancer U251, SF-268, SF-295, SF-539, SNB-75, and SNB-78; colon cancer HCC2998, KM-12, HT-29, HCT-15, and HCT-116; lung cancer NCI-H23, NCI-H226, NCI-H522, NCI-H460, A549, DMS273, and DMS114; melanoma LOX-IMVI; ovarian cancer OVCAR-3, OVCAR-4, OVCAR-5, OVCAR-8, SK-OV-3; renal cancer RXF-631L and ACHN; stomach cancer St-4, MKN1, MKN7, MKN28, MKN45, and MKN74; prostate cancer DU-145 and PC-3. The GI_{50} values for these cell lines were determined by using the sulforhodamine B colorimetric method [9].

REFERENCES

[1] M. Kikuchi, Y. Yamauchi, C. Yanase, I. Nagaoka, *Yakugaku Zasshi* **1987**, *107*, 245.
[2] K. Ishiguro, M. Yamaki, S. Takagi, Y. Ikeda, K. Kawakami, K. Ito, T. Nose, *Chem. Pharm. Bull.* **1986**, *34*, 2375.
[3] K. Konno, C. Hirayama, H. Yasui, M. Nakamura, *Proc. Natl. Acad. Sci. U.S.A.* **1999**, *96*, 9159.
[4] M. Guiso, C. Marra, *Nat. Prod. Res.* **2005**, *19*, 105.
[5] L. J. El-Naggar, J. L. Beal, *J. Nat. Prod.* **1980**, *43*, 649.
[6] P. Gariboldi, G. Jommi, L. Verotta, *Phytochemistry* **1986**, *25*, 865.
[7] S. P. Shrestha, Y. Narukawa, T. Takeda, *J. Nat. Med.* **2007**, *61*, 73.
[8] T. Tanahashi, Y. Takenaka, N. Okazaki, M. Koge, N. Nagakura, T. Nishi, *Phytochemistry* **2009**, *70*, 2072.
[9] T. Yamori, A. Matsunaga, S. Sato, K. Yamazaki, A. Komi, K. Ishizu, I. Mita, H. Edatsugi, Y. Matsuba, K. Takezawa, O. Nakanishi, H. Kohno, Y. Nakajima, H. Komatsu, T. Andoh, T. Tsuruo, *Cancer Res.* **1999**, *59*, 4042.
[10] K. D. Paull, R. H. Shoemaker, L. Hodes, A. Monks, D. A. Scudiero, L. Rubinstein, J. Plowman, M. R. Boyd, *J. Natl. Cancer Inst.* **1989**, *81*, 1088.

Received April 6, 2010